Development 124, 2935-2944 (1997)
Printed in Great Britain © The Company of Biologists Limited 1997
DEV4870

Lhx2, a LIM homeobox gene, is required for eye, forebrain, and definitive erythrocyte development

Forbes D. Porter[1,*], John Drago[3,*], Yang Xu[4], Surindar S. Cheema[3], Chris Wassif[1], Sing-Ping Huang[2], Eric Lee[2], Alexander Grinberg[2], Jim S. Massalas[3], David Bodine[5], Frederick Alt[4] and Heiner Westphal[2]

[1]Heritable Disorders Branch, National Institutes of Health, Bethesda, MD 20892, USA
[2]Laboratory of Mammalian Genes and Development, National Institutes of Health, Bethesda, MD 20892, USA
[3]Department of Anatomy, Monash University, Clayton, 3168 Victoria, Australia
[4]Howard Hughes Medical Institute, The Children's Hospital and Department of Genetics Center for Blood Research, Harvard Medical School, Boston, MA 02115, USA
[5]Laboratory of Gene Transfer, National Institutes of Health, Bethesda, MD 20892, USA

*Co-first authors
e-mail: fdporter@helix.nih.gov

SUMMARY

We investigated the function of *Lhx2*, a LIM homeobox gene expressed in developing B-cells, forebrain and neural retina, by analyzing embryos deficient in functional Lhx2 protein. *Lhx2* mutant embryos are anophthalmic, have malformations of the cerebral cortex, and die in utero due to severe anemia. In *Lhx2–/–* embryos specification of the optic vesicle occurs; however, development of the eye arrests prior to formation of an optic cup. Deficient cellular proliferation in the forebrain results in hypoplasia of the neocortex and aplasia of the hippocampal anlagen. In addition to the central nervous system malformations, a cell non-autonomous defect of definitive erythropoiesis causes severe anemia in *Lhx2–/–* embryos. Thus *Lhx2* is necessary for normal development of the eye, cerebral cortex, and efficient definitive erythropoiesis.

Key words: LIM homeobox, eye, forebrain, erythropoiesis, mouse

INTRODUCTION

Transcription factors containing homeodomains play a major role in morphogenesis. The homeodomain is a highly conserved protein motif that binds DNA, and homeodomain proteins function as cell specific transcription factors. In addition to the prototypical homeobox genes characterized by the paralogous HoxA-D clusters, multiple sub-families of homeobox genes exist. These families have distinct homeodomains and often are found in association with other protein motifs (Gehring et al., 1994; Manak and Scott, 1994). The LIM homeodomain encoding genes are one of these families.

LIM homeobox genes encode a LIM type homeodomain and two zinc-finger like LIM domains. Recent reviews (Dawid et al., 1995; Sánchez-García and Rabbitts, 1994) describe the structure, function and nomenclature of LIM domain and the LIM homeodomain families. LIM domains bind zinc ions (Archer et al., 1994), and nuclear magnetic resonance studies showed that LIM domains have a secondary structure similar to the DNA binding domains of both the glucocorticoid receptor and GATA-1 (Perez-Alvarado et al., 1994). Unlike these zinc-finger containing transcription factors, LIM domains do not interact directly with DNA. Instead LIM domains are involved in protein-protein interactions (Crawford et al. 1992; Feuerstein et al., 1994; Schmeichel and Beckerle, 1994; Wadman et al., 1994; Wu and Gill, 1994; Agulnick et al., 1996; Jurata et al. 1996), and may modulate the function of the homeodomain (German et al., 1992; Sánchez-García et al., 1993; Xue et al., 1993; Taira et al., 1994; Agulnick et al., 1996).

The LIM homeobox genes are expressed widely in the developing central nervous system, and may be involved in specification of neurons. In the ventral spinal cord, pairs of LIM homeobox genes are expressed in specific subsets of motor neurons (Tsuchida et al., 1994). In the developing forebrain and hindbrain, specific domains of expression are reported for *Lhx1* (LIM-1) (Barnes et al., 1994; Fujii et al., 1994), *Lhx2* (LH-2) (Xu et al., 1993), *Lhx3* (mLIM-3; pLIM) (Bach et al., 1995; Seidah et al., 1994; Zhadanov et al., 1995), *Lhx4* (GSH-4) (Li et al., 1994), *Lhx5* (LIM-2) (Sheng et al., 1997), and *Isl-1* (Thor et al., 1991). The observations that *Lhx4* mutant mice die during the perinatal period reportedly due to abnormal brainstem regulation of respiratory drive (Li et al., 1994), and that *Isl1–/–* mice have abnormal development of motor neurons in the ventral spinal cord (Pfaff et al., 1996) demonstrate the functional importance of LIM homeobox genes in CNS development.

LIM homeobox genes are required for morphogenesis of other organ systems. *Lhx1* is required for renal and gonadal development, as well as prechordal mesoderm formation (Shawlot and Behringer, 1995). *Lhx3* and *Lhx4* are necessary for normal pituitary development (Sheng and Westphal; unpub-

lished data). *Lmx1* appears to play a role in dorsal-ventral patterning of the chicken wing (Riddle et al., 1995; Vogel et al., 1995).

Lhx2, formerly *LH-2*, was cloned from a pre-B cell library subtracted against a B-cell library (Xu et al., 1993). *Lhx2* was also independently cloned by Robertson et al. (1994) as a factor that bound to the glycoprotein hormone α-subunit promoter. *Lhx2* is not only expressed in preB-cells and B-cells, but is also expressed in γδT-cells and the developing central nervous system. In rat embryos, *Lhx2* transcripts were first observed on embryonic day 11 (E11) and by E12-13 there was strong expression in cells surrounding the telencephalic ventricles, in the diencephalon and in the marginal layer of the myelencephalon. At the time of birth, *Lhx2* probes intensely hybridize to cortical layers 2-6, and central nervous system expression persists into adulthood (Xu et al., 1993). To determine the essential functions of *Lhx2* in development, we inactivated the *Lhx2* gene by homologous recombination in embryonic stem cells. These experiments show that *Lhx2* is required for normal development of the eye, cerebral cortex and definitive erythrocytes.

MATERIALS AND METHODS

Disruption of the *Lhx2* allele by homologous recombination in embryonic stem cells

The targeting vector (pEGneo) was constructed as described by Wu and Alt (in preparation). pEGneo (25 mcg) was linearized with *Xba*I, and electroporated (BioRad Electroporator, 400 V, 25 μF) into J1 embryonic stem (ES) cells (Li et al., 1992). Electroporated ES cells were plated at a density of 2.5×10^5 cells in 60 mm^2 dishes containing a layer of G418 resistant embryonic fibroblasts. Selection for G418 resistant (400 mcg/ml, Gibco BRL) and gancyclovir (2 μM, Syntex) resistant colonies was begun 24 hours after plating. Double resistant colonies were isolated and expanded after 5 days of selection. DNA was prepared as previously described (Laird et al., 1991).

Genotyping of ES cell clones and *Lhx2–/–* mice

Southern blot analyses of individual clones were performed using standard procedures. Genomic DNA was digested overnight with either *Xba*I or *Hin*dIII, separated on a 0.8% TAE agarose gel, and transferred onto Gene Screen Plus (NEN Research Products) membranes. The probe shown in Fig. 1A was labeled using a random primed DNA labeling kit (Boehringer Mannheim). Autoradiographs were utilized to identify the wild-type and mutant alleles as demonstrated in Fig. 1B. *Lhx2*+/– ES clones were injected into C57/B6 blastocysts as previously described (Bradley, 1987). Progeny with a *Lhx2*+/– genotype were identified by Southern blot analysis of tail biopsy genomic DNA. For timed matings, the identification of a copulatory plug was considered to be E0.5, and embryonic age was confirmed by inspection. Southern blot analysis of yolk sac DNA was used to genotype embryos.

Histological techniques, volumetric analysis, and in situ hybridization

Hematoxylin and eosin, TUNEL, and Cresyl violet staining was performed on embryos fixed in Bouin's fixative, paraffin embedded, and sectioned (5 μm) in the indicated orientation. In situ analysis was as previously described (Mackem and Mahon, 1991). For BrdU labeling, pregnant heterozygous females, E12.5, were injected with 0.1 mg of BrdU (Sigma #B5002, at a stock concentration of 10 mg/ml) per gram of body weight, and embryos were harvested 2 hours postinjection. Embryos were immersion fixed in Bouin's fixative, and then paraffin embedded. 8 μm sections were cut in the coronal plane, mounted on AES-coated glass slides, and immunostained using a 1 in 400 dilution of anti-BrdU antiserum (Sigma #P2531) followed by a biotin-conjugated horse anti-mouse second antibody. A Vectorstain Elite kit (Vector Laboratories) was used for final antigen detection using DAB and hydrogen peroxide. The DAB reaction product was intensified in 0.01% osmium tetroxide, and counter stained with hematoxylin. Due to the forebrain malformation in mutants, an exact match of control and mutant sections was precluded. Sections that showed a prominent basal ganglionic bulge, an obvious cortical plate, prominent lateral ventricles, and a midline III ventricle contour were selected as the best match for determining the BrdU labeling index and morphological assessment. For volumetric analysis, paraffin blocks were serially sectioned (8 μm), and every fifth section was stained for analysis. Tracings of the central nervous system were made using a projection microscope at a final magnification of 35×. Morphometric analyses were made using a computer linked image analysis system.

Hematological analysis

For determination of hematocrits, embryos were isolated, blotted dry and blood was collected from the umbilicus in a pyrex microcapillary tube previously treated with sodium citrate. The microcapillary tube was inserted into a standard hematocrit tube and centrifuged in a IEC microhematocrit machine. Methyl cellulose assays were performed in MethoCult M3430 (Stem Cell Technologies Inc.) following the manufacturers instructions. *Lhx2–/–* ES stem cells were obtained by exposing *Lhx2*+/– ES cells to elevated concentrations of G418 (Xu and Alt, unpublished), and chimeric animals were produced as described above. Hemoglobin analysis was as previously described (Whitney, 1978).

Fetal liver transplant and flow cytometric analysis of hematopoietic cells

Fetal livers were recovered from E13.5 embryos and disrupted by teasing between the frosted ends of two microscope slides. The single cell suspension was filtered through nylon mesh and a small fraction of these cells were genotyped. Five million *Lhx2–/–* and *Lhx2*+/+ fetal liver cells were injected intravenously into irradiated C57BL6 mice. Recipient mice were irradiated twice with split doses of 800 and 400 rads. For flow cytometric analysis single cell suspensions were prepared from thymus, spleen and bone marrow as previously described (Xu et al., 1996). 500,000 cells were stained in each reaction. Stained cells were analyzed with a FACSscan (Becton-Dickinson) using the CellQuest software. PE-conjugated anti-CD4, anti-B220 antibodies, FITC-conjugated anti-CD8 antibody, and biotinylated anti-Ter 119 and anti-CD43 antibodies were obtained from Pharmingen. Biotinylated anti-Gr-1 antibody was obtained from Southern Biotechnology Associate, Inc. Biotinylated derivatives were revealed with FITC-conjugated streptavidin.

RESULTS

Targeted disruption of *Lhx2*

We inactivated the *Lhx2* gene using homologous recombination in embryonic stem cells (ES cells). A replacement targeting vector, pEGneo, was designed to delete the two exons encoding the LIM domains and the domain linking the LIM domains and homeodomain of *Lhx2*, and replace them with a neomycin-resistance gene (*PGK-neo*). Potential splicing between exons one and four would introduce a frameshift mutation that would preclude expression of a homeodomain containing peptide. We used herpes simplex thymidine kinase, under control of the phosphoglycerate kinase promoter (*PGK-*

tk), to select against random insertion events (Mansour et al., 1988). Fig. 1A illustrates a partial genomic restriction map of *Lhx2*, our targeting strategy, and the probe (G11) used to identify properly targeted ES cell clones. Digestion of genomic DNA from G418/gancyclovir double-resistant clones with *Xba*I followed by Southern blot analysis established that homologous recombination occurred in both the 5′ and 3′ flanks of the targeting vector. Fig. 1B demonstrates the presence of the 18 kb targeted and the 6 kb normal allele in two independent clones (F6 and F101). Southern blot analysis confirmed a single insertion of the PGK-neo construct in both clones (data not shown). Both clones produced germline transmitting chimeras after injection into C57BL/6 blastocysts.

Heterozygous *Lhx2* mutant mice were phenotypically normal, thus we intercrossed *Lhx2*+/– mice to determine if the *Lhx2* mutant allele had a recessive phenotype. Genotyping of 191 weaned offspring of these matings identified 71 *Lhx2*+/+ (37%) and 120 *Lhx2*+/– (63%) progeny, but no *Lhx2*–/– mice. Some stillborn *Lhx2*–/– pups were found. Genotyping of 242 embryos, E15.5 and younger, yielded numbers closer to the expected Mendelian ratio for an autosomal recessive mutation (+/+ 24%, +/– 55%, –/– 21%). Fig. 1C shows the genotyping of these embryos and the presence of homozygous mutant embryos. The lower than expected number of homozygous mutant embryos may represent early in utero death of some *Lhx2*–/– embryos. When reabsorbing embryos were genotyped, a disproportionately high number of homozygous mutants were found (data not shown). Likewise, the *Lhx2* mutation was recessive and embryonic lethal on an inbred 129/Sv background.

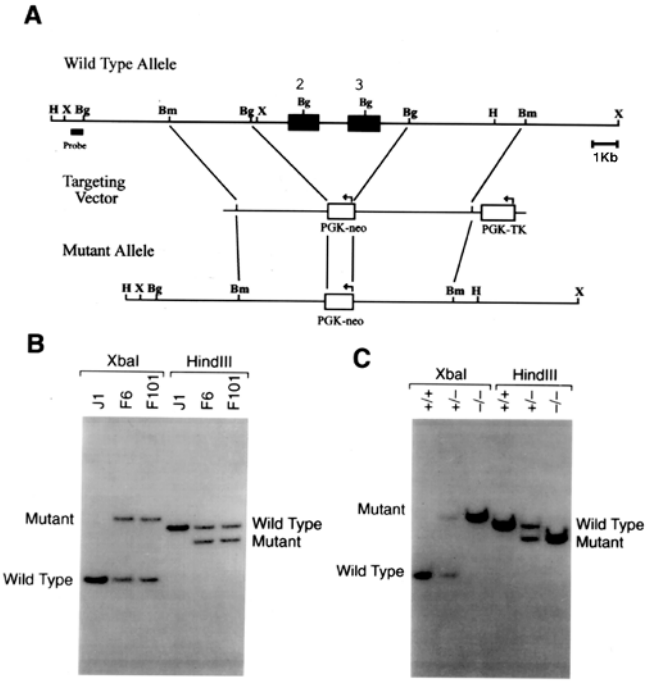

Fig. 1. *Lhx2* targeting strategy and genotyping. (A) A restriction map of the genomic region containing the *Lhx2* gene is shown at the top with exons numbered (position, but not size indicated by the dark boxes). The targeting vector is shown in the middle, and the targeted allele is shown at the bottom. Using *Xba*I digestion of genomic DNA, the wild-type (6 kb) or the targeted allele (18) can be distinguished using the external probe located at the 5′ end of the gene. Restriction sites are abbreviated as follows: *Hin*dIII (H), *Xba*I (X), *Bgl*II (Bg), and *Bam*HI (B). (B) Southern blot analysis of genomic DNA from two independently targeted embryonic stem cell lines (F6 and F101), and from the parental embryonic stem cell line J1. The wild-type and the targeted allele could be distinguished by a restriction fragment length polymorphism using either *Xba*I or *Hin*dIII digested genomic DNA, and the external probe diagrammed above. (C) Genotyping of E13.5 embryos from a *Lhx2*+/– intercross. Both *Xba*I and *Hin*dIII restriction fragment length polymorphisms identified by Southern blot analysis were used to genotype embryos from a *Lhx2*+/– intercross.

We observed three major phenotypic abnormalities in E13.5 *Lhx2*–/– embryos. They were anophthalmic, had flattening of the forehead region due to cerebral cortex abnormalities, and had small livers (Fig. 2). After E13.5 the *Lhx2*–/– embryos were notably paler than their littermates. Stillborn pups were pale and hydropic. The observations that the *Lhx2*–/– embryos were pale, hydropic, and had small fetal livers suggested that the in utero death was due to a defect in definitive erythropoiesis.

Lhx2 is necessary for eye development

Using in situ analysis, we observed *Lhx2* expression in the region of the optic vesicle as early as E8.5 (data not shown). Prior to birth we saw *Lhx2* expression throughout the neural retina; while postnatally, *Lhx2* expression became restricted to the inner nuclear layer of the retina (Xu et al., 1993; data not shown). Mice homozygous for the *Lhx2* mutant allele were anophthalmic. By E13.5 no lens, globe, or retina were seen in *Lhx2*–/– embryos (Fig. 3A,B). However, the eyelid folds and, in some older embryos, the extraocular muscles persisted. Analysis of hematoxylin and eosin stained sections from E9.5 embryos demonstrated that eye development arrested after formation of an optic vesicle but prior to formation of an optic cup (Fig. 3C,D). Eye development did not proceed further in the mutant embryos, and by E10.5 only a small remnant of the optic vesicle was observed (data not shown).

Mice with mutations in *Pax6* (Sey) are anophthalmic (Hill et al., 1991) and *Pax6* has been hypothesized to be a ‘master control gene’ for eye development (Halder et al., 1995). We thus hypothesized that a regulatory relationship between *Pax6* and *Lhx2* might exist. Using in situ hybridization analysis, we found that *Pax6* continued to be expressed in the arrested optic vesicle of *Lhx2*–/– embryos. Fig. 3E demonstrates *Pax6* expression in the nascent optic vesicle of a E9.5 *Lhx2*+/+ embryo, while Fig. 3F shows the persistence of *Pax6* expression in the arrested optic vesicle of a *Lhx2*–/– littermate. Conversely, homozygous Sey embryos continue to express *Lhx2* in the developing optic vesicle/cup (Richard Maas, personal communication). *Pax6* is also normally expressed in the lens placode (Hill et al., 1991; Walther and Gruss, 1991). We did not observe a lens placode in hematoxylin and eosin stained sections from *Lhx2*–/– embryos (Fig. 3D), and we did not see specific hybridization of a *Pax6* probe to the ectoderm overlying the arrested optic vesicle of *Lhx2*–/– embryos (Fig. 3F).

Lhx2 is necessary for efficient definitive erythropoiesis

We found a significant decrease in the hematocrits of *Lhx2*–/– embryos between E13.5 and E15.5 (Fig. 4A). *Lhx2*+/+ and +/–

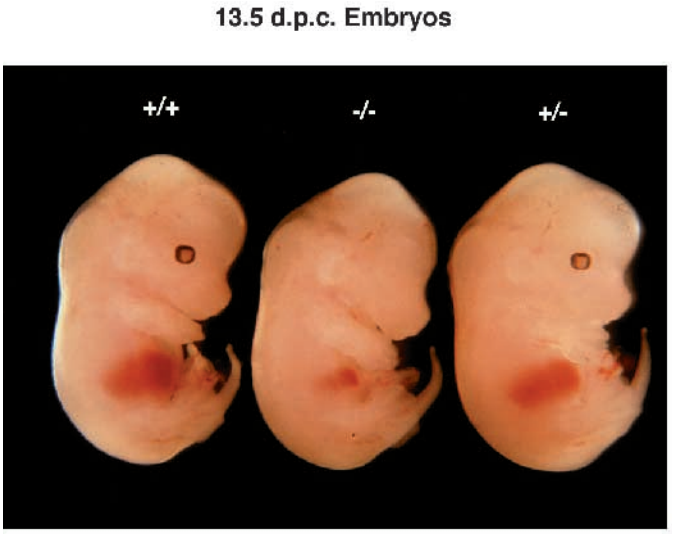

Fig. 2. Phenotypic comparison of E13.5 littermates from a *Lhx2*+/– intercross. A *Lhx2*+/+ embryo is shown on the left, a heterozygous embryo is shown on the right, and a *Lhx2*–/– embryo is shown in the middle. Anophthalmia, flattening of the forehead region, and a small liver are seen in the mutant embryos.

embryos had hematocrits in the 30-40% range; however, by E15 the hematocrits of *Lhx2*–/– mice decreased to about 10%. This time course was consistent with normal yolk sac erythropoiesis, but impaired definitive erythropoiesis (Russell, 1979).

Definitive erythropoiesis was not completely blocked in the mutant embryos. Microscopic analysis of Wright-Giemsa stained blood smears from E12.5-E15.5 embryos showed that mature enucleated erythrocytes were present in *Lhx2*–/– embryos (Fig. 4C). However, we did note variation in the size of the *Lhx2*–/– erythrocytes. The percentage of enucleated erythrocytes in *Lhx2*–/– embryos progressively increased from E12.5 to E15.5 (Fig. 4B). Thus, although the hematocrit of mutant embryos was severely reduced by E15.5, mature erythrocytes were the most common type of erythrocytes present in the mutant embryos. Although *Lhx2*–/– livers were smaller than normal, histological examination of liver sections stained with hematoxylin and eosin demonstrated hematopoietic foci of normal appearance in the parenchyma of the mutant livers (data not shown). Thus definitive erythropoiesis was inefficient rather than completely blocked in the mutant embryos.

Methylcellulose colony-forming assays, which allowed quantitation of erythrocyte progenitor cells in fetal livers, were undertaken to further characterize the erythropoietic defect. Similar results were observed with *Lhx2*+/+ and +/– embryos, thus these data were combined. Per 100,000 nucleated cells, there was a significant reduction of two types of erythrocytic precursors (Fig. 5). Blast Forming Unit-erythroid progenitors (BFU-e), the earliest pure erythrocytic precursor, and Colony Forming Unit-erythroid progenitors (CFU-e), a more mature erythrocytic precursor, were both significantly decreased in the mutant livers. In contrast, the number of Colony Forming Unit-Granulocyte/Macrophage progenitors (CFU-GM) was not significantly reduced (Fig. 5). Enumeration of nucleated cells from control and mutant livers demonstrated a seven-fold reduction in the cellularity of the *Lhx2*–/– livers (11.5×10^6 versus 1.6×10^6). Therefore, the total numbers, per liver from

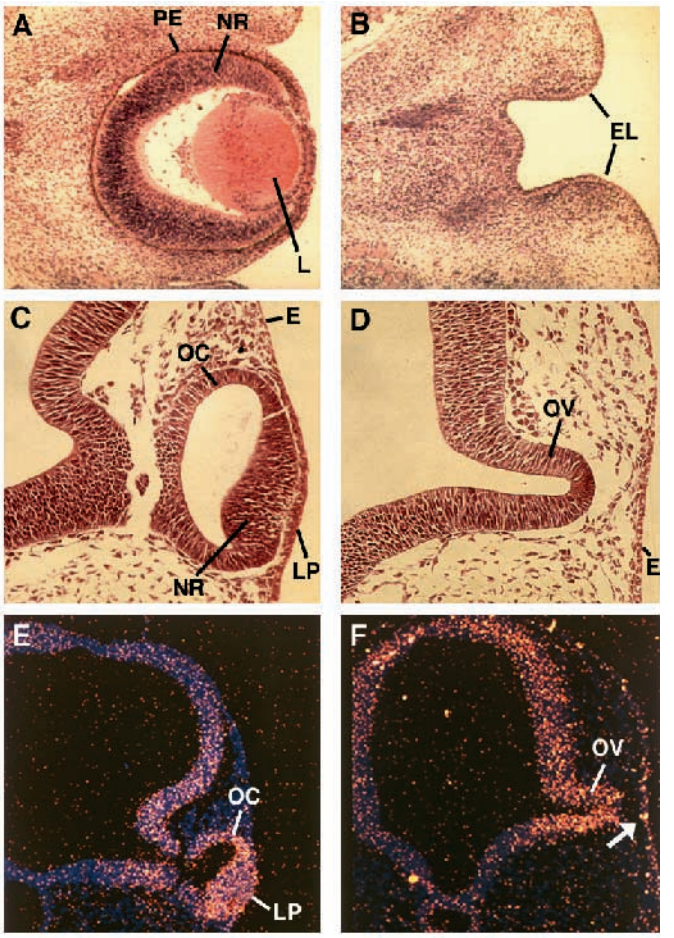

Fig. 3. Sections from the eye region and *Pax6* in situ analysis. (A) Hematoxylin and eosin stained section from an E13.5 *Lhx2*+/+ embryo. A well formed eye including pigmented epithelium (PE), neural retina (NR) and a lens (L) is observed at this point in development. (B) Hematoxylin and eosin stained section from an E13.5 *Lhx2*–/– embryo. Structures derived from the optic vesicle and the lens are absent. Primordial eyelids (EL) are present, and will subsequently fuse to form a conjunctival sac. Magnification is the same as in A. (C) Hematoxylin and eosin stained section from an E9.5 *Lhx2*+/+ embryo. The optic vesicle is beginning to invaginate to form the optic cup (OC), and the ectoderm (E) overlying the optic vesicle begins to thicken to form the lens placode (LP). The neural retina (NR) is also labeled. (D) Hematoxylin and Eosin stained section from an E9.5 *Lhx2*–/– embryo. Development of the eye arrests after formation of the optic vesicle (OV), but prior to formation of the optic cup. Thickening of the ectoderm (E) to form a lens placode is not observed. Magnification is the same as in (C). (E) *Pax6* expression in an E9.5 *Lhx2*+/+ embryo. In situ analysis demonstrated *Pax6* expression in the developing optic cup (OC) and the lens placode (LP) of an *Lhx2*+/+ embryo. (F) *Pax6* expression in a E9.5 *Lhx2*–/– embryo. In situ analysis of *Pax6* expression in a *Lhx2*–/– embryo showed expression of *Pax6* in the arrested optic vesicle (OV) but no specific hybridization to the overlying ectoderm was seen (arrow).

Lhx2–/– embryos, of BFU-e and CFU-e progenitor cells were reduced 16-fold and 40-fold respectively. In contrast, the reduction (eight-fold) in the number of CFU-GM progenitor cells was proportional to the reduction in total liver cellularity. The multipotent progenitor cells, Colony Forming Unit-Gran-

ulocyte/Erythrocyte/Macrophage (CFU-GEM), that give rise to both erythrocytic and myelocytic lineages were reduced 16-fold in the *Lhx2–/–* livers. However, a possible defect in the production of erythrocytes would impair our ability to identify CFU-GEM progenitors from mutant embryos. If the erythrocytic component of a multipotent CFU-GEM did not develop normally, these colonies would be enumerated as CFU-GM colonies. Thus, a firm conclusion about the status of the CFU-GEM progenitor cells was precluded.

The erythrocytic defect observed in *Lhx2–/–* embryos could have been due to an intrinsic defect in the development of the erythrocytic lineage itself (cell autonomous) or due to an extrinsic defect in the surrounding microenvironment (cell non-autonomous). To distinguish between these two possibilities we analyzed *Lhx2* chimeric mice. We obtained a *Lhx2–/–* embryonic stem cell clone by exposing *Lhx2+/–* embryonic stem cells to elevated concentrations of G418 (Wu and Alt, unpublished). These *Lhx2–/–* embryonic stem cells were injected into C57BL/6 blastocysts to produce chimeric animals. The embryonic stem cells were derived from a 129/Sv mouse, thus erythrocytes derived from these cells express the hemoglobin-diffuse (Hb-d) allele; whereas, erythrocytes derived from C57BL/6 cells express the hemoglobin-single (Hb-s) allele. We took advantage of this hemoglobin polymorphism in order to determine the ability of *Lhx2–/–* embryonic stem cells to contribute to definitive erythropoiesis in chimeric animals. Our results are tabulated in Table 1. *Lhx2–/–* embryonic stem cells retained the ability to significantly contribute to erythropoiesis in chimeric animals. In seven highly chimeric animals, the level of Hb–d ranged from 40-80%. None of these chimeras were hydropic or pale. Thus, the effect of *Lhx2* on erythropoiesis was cell non-autonomous. In contrast, given the high frequency of microphthalmia and anophthalmia seen in these chimeric pups, the effect of *Lhx2* on eye development was judged to be cell autonomous.

To confirm the cell nonautonomous nature of the erythropoietic defect, fetal liver cells from *Lhx2+/+* and *Lhx2–/–* embryos were transplanted into lethally irradiated recipient mice. Flow cytometric analysis was used to study the development of various hematopoietic lineages in these 'reconstituted mice'. The cellular composition of the thymus and spleens of the mice reconstituted with *Lhx2–/–* fetal liver cells is similar to those of mice reconstituted with *Lhx2+/+* fetal liver cells (Fig. 6A,B, data not shown). Furthermore, analysis of pro/pre-B (Fig. 6C), granulocytic (Fig. 6D) and erythroid (Fig. 6D) lineages in the bone marrow of mice reconstituted with *Lhx2* mutant cells did not show any defects. These findings indicate that Lhx2 is not required for the development these hematopoietic lineages. The Ter-119 data confirm the hemoglobin chimeric data presented above, and demonstrate that the erythropoietic defect seen in *Lhx2–/–* embryos is due to a defective fetal liver microenvironment.

Hypoplasia of the cerebral cortex and agenesis of the hippocampal anlagen is present in *Lhx2–/–* embryos

Analysis showed marked reduction of the size of the forebrain in *Lhx2–/–* embryos older than E12.5. Reliable differences in the telencephalic contours are not seen prior to E12.5. Sections from E13.5 mutant embryos stained with hematoxylin and eosin (data not shown) or cresyl fast violet showed agenesis of the hippocampal anlagen, hypoplasia of the cortical plate and hypoplasia of the basal ganglia (Fig. 7A-D). We performed morphometric analysis to determine the relative sizes of the forebrain, basal ganglia, cortical plate, ventricular compart-

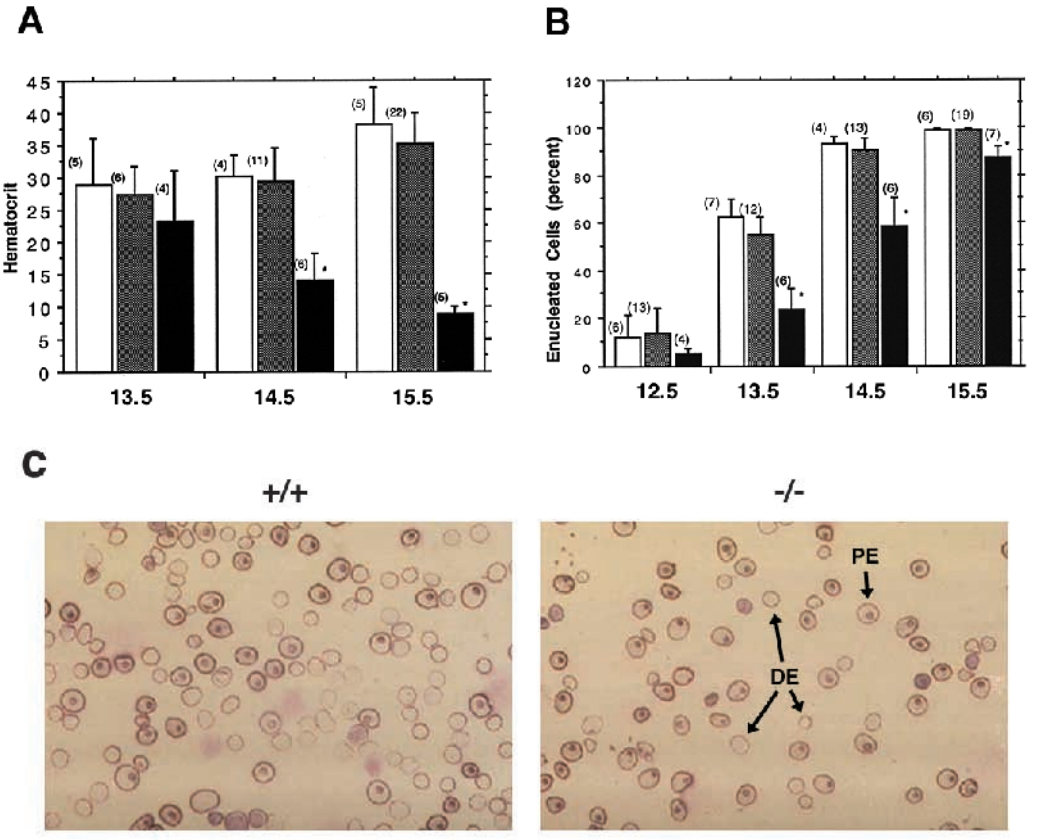

Fig. 4. Blood analysis of progeny from *Lhx2+/–* matings. Hematocrits (A) and the percentage of enucleated erythrocytes (B) from *Lhx2+/+* (□), +/– (▩), and –/– (■) embryos were measured at the indicated gestational ages. The error bars represent one standard deviation. *Indicates $P<0.001$ using a Student *t*-test. The number of embryos analyzed is indicated, in parenthesis, at the top of each bar. (C) Wright-Giemsa stained peripheral blood smears from *Lhx2+/+* and –/– embryos. Yolk sac derived (PE) and hepatic derived (DE) erythrocytes are observed in both embryos.

Table 1. Chimeric analysis

Pup	Eye phenotype	Hemoglobin (%) Hb-s	Hb-d
1	Anophthalmic	33	63
2	Normal	31	69
3	Normal	97	3
4	Normal	20	80
5	Left: anophthalmia		
	Right: microphthalmia	40	60
6	Left: normal		
	Right: microphthalmia	40	60
7	Normal	60	40
8	Normal	50	50

Lhx2–/– embryonic stem cells were injected into C57BL/6 blastocysts. The resulting chimeric pups were examined for ocular abnormalities, and the percentage of each hemoglobin variant was determined.

ment, hippocampus and the diencephalon between *Lhx2*+/+ and *Lhx2–/–* embryos (Fig. 8). The most severe effect of the *Lhx2* mutation on brain development was agenesis of the hippocampus; however, cortical plate and basal ganglia volumes were significantly reduced. In contrast, the diencephalon appeared normal both qualitatively and quantitatively (Figs 7A,B, 8). Similar results were observed with E13.5 embryos (data not shown).

Examination of the ventricular region of *Lhx2–/–* embryos revealed an apparent decrease in the number of mitotic figures compared to *Lhx2*+/+ embryos (data not shown). This suggested that the cerebral cortex hypoplasia resulted from decreased proliferation of neural precursors. To confirm the accuracy of this observation, we performed BrdU staining of the brain from *Lhx2–/–* and *Lhx2*+/+ embryos exposed to a pulse of BrdU. BrdU-positive cells from both *Lhx2*+/+ and *Lhx2–/–* embryos stained to the same degree; however, we found that the number of BrdU positive cells in the developing cerebral cortex of *Lhx2–/–* embryos was markedly reduced (Fig. 7E,F). A labeling index was derived from two distinct sites of the developing cerebral cortex. The labeling index

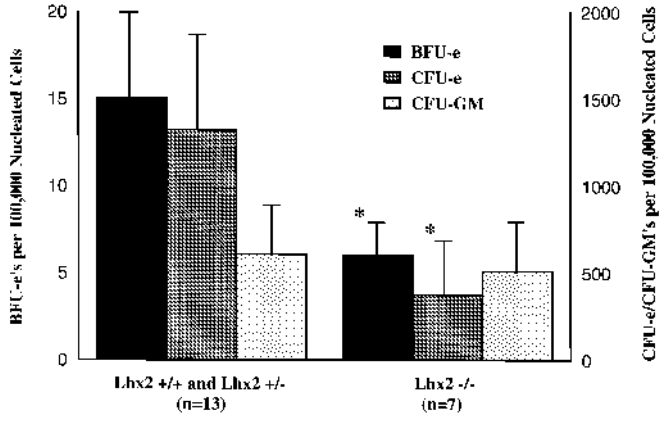

Fig. 5. Methylcellulose colony-assay of hematopoietic progenitor cells. CFU-e, BFU-e, and CFU-GM progenitor cells, per 100,000 nucleated cells, from E13.5 control (*Lhx2*+/+ and +/–) embryos, and *Lhx2–/–* embryos were enumerated. The *Lhx2–/–* had a significant reduction (P<0.001) in the number of CFU-e and BFU-e progenitor cells. Error bars represent one standard deviation.

within the superomedial cerebral cortex for control embryos was 0.29±0.06 (n=8) and for *Lhx2* mutant embryos was 0.13±0.02 (n=6). The superolateral cortex values were 0.33±0.02 for controls and 0.15±0.02 for mutant embryos. Counts were bilaterally derived and were statistically significant (P<0.001). Analysis for cell death using the TUNEL stain in E13.5 embryos did not reveal any difference between mutant and control brains (data not shown). These data confirmed that the hypoplasia of the cerebral cortex was primarily due to a defect in precursor cell proliferation.

DISCUSSION

Targeted disruption of *Lhx2*, a LIM homeobox gene

We produced a functionless *Lhx2* allele by homologous recombination in embryonic stem cells using a standard positive/negative targeting strategy. *Lhx2*+/– mice were phenotypically normal; however, *Lhx2–/–* embryos were anophthalmic, had forebrain malformations and were anemic. Thus *Lhx2* plays an essential role in the development of the eye, the forebrain and definitive erythrocytes.

Lhx2 is essential for eye development

Eye development in the mouse begins on E8 with outgrowth of the optic vesicle from the neuroepithelium. On E9, the optic vesicle contacts the overlying ectoderm and begins to invaginate to form the optic cup. The inner layer of the optic cup will proliferate and give rise to the multi-layered neural retina; whereas, the outer layer of the optic cup will remain as a single cellular layer and become the retinal pigment epithelial layer. Concurrently, the overlying surface ectoderm thickens to form the lens placode, and then subsequently invaginates to form the lens vesicle. A series of reciprocal inductive interactions between the optic cup and lens vesicle are thought to control the development of the eye (Grainger, 1992; Saha et al., 1992).

Lhx2 expression has been observed in the optic vesicle as early as E8.5, and is highly expressed throughout the neural retina during embryonic development. Postnatally, expression of *Lhx2* becomes restricted to the inner nuclear layer. This study has shown that *Lhx2* is essential for progression of the optic vesicle to the optic cup stage. Specification of the optic vesicle in *Lhx2–/–* embryos appears normal; however, eye development arrests prior to formation of the optic cup. Thus *Lhx2* is essential for proper outgrowth and invagination of the optic vesicle to form the optic cup.

Given this early defect in eye development, we were interested in determining whether *Lhx2* was necessary for the expression of other genes important for eye development. One such gene is *Pax6*. *Pax6* is normally expressed in both the lens placode and the optic vesicle. The *Drosophila* homolog of *Pax6*, *eyeless*, functions as a master regulatory gene for eye development (Halder et al., 1995), and mutations of *Pax6* have been found in the *Small eye* (*Sey*) mouse and in cases of human aniridia (Hanson and van Heyningen, 1995). Eye development in the Sey mouse arrests after outgrowth of the optic vesicle (Hogan et al., 1986). Thus, conceivably, *Lhx2* could regulate *Pax6* expression in the developing eye. We found, using in situ analysis, that *Pax6* expression continued in the arrested optic vesicles of *Lhx2–/–* embryos. Conversely, *Lhx2* expression has been reported to be normal in *Sey* mice. These results suggest

that *Lhx2* and *Pax6* are independently essential for normal development of the optic vesicle and cup.

In contrast to the continued expression of *Pax6* in the mutant optic vesicles, *Pax6* expression in the ectoderm overlying the optic vesicle was not observed in *Lhx2–/–* embryos. We observed *Pax6* expression in the lens placode of *Lhx2+/+* embryos; however, we did not observe specific hybridization of a *Pax6* probe in the ectoderm overlying the arrested optic vesicle of *Lhx2–/–* embryos. These data suggest that *Lhx2* function in the optic vesicle is necessary for either induction or maintenance of *Pax6* expression in the presumptive lens ectoderm.

Definitive erythropoiesis is inefficient in *Lhx2* mutant embryos

Erythrocyte development occurs in two distinct phases. In the mouse, primitive erythropoiesis is first observed on E7 in blood islands of the yolk sac. By E12, the major site of erythropoiesis shifts from the yolk sac to the fetal liver following migration of pluripotent hematopoietic stem cells into the fetal liver. The erythrocytes formed in the embryonic liver are distinct from primitive erythrocytes and are similar to those formed in the bone marrow. This phase of erythropoiesis is referred to as definitive erythropoiesis. The fetal liver remains the major site of erythropoiesis until after E15 when it shifts initially to the spleen and subsequently to the bone marrow (Russell, 1979).

Erythropoiesis appeared normal in *Lhx2–/–* embryos prior to E12; however, these embryos had a significant drop in their hematocrits between E13 and E15. This suggested a problem in definitive erythropoiesis. The fall in hematocrit could have been the result of either decreased erythrocyte formation, or increased erythrocyte destruction. The decreased liver size of *Lhx2–/–* embryos suggested a failure in erythrocyte production, and the decrease in erythrocyte progenitor cells confirmed that the anemia in the mutant mice was due to abnormal production of erythrocytes rather than increased destruction. By E15.5 most of the erythrocytes in *Lhx2–/–* embryos were of the mature type; however, their number, as reflected by the hematocrit, was significantly decreased. Thus definitive erythropoiesis was inefficient in *Lhx2–/–* embryos rather than completely blocked.

To further define *Lhx2* function in hematopoiesis, methylcellulose cultures of hematopoietic progenitor cells from fetal liver were performed. *Lhx2–/–* embryos had a seven-fold reduction in the absolute number of nucleated cells present in E13.5 livers, and compared to control animals, *Lhx2–/–* embryos had a 16-fold decrease in BFU-e and a 40-fold decrease in CFU-e progenitor cells. In comparison, the decrease in the number of CFU-GM progenitor cells (8-fold) was just proportional to the decrease in total cellularity (7-fold). Thus, the lack of *Lhx2* function had a disproportionate effect on erythropoiesis, and in particular impaired the progression of BFU-e to CFU-e progenitors.

A defect in the hepatic phase of erythropoiesis could be due to several causes. Either the migration of pluripotent hematopoietic stem cells to the fetal liver, the maturation of a multipotent progenitor cell, or the maturation of a lineage restricted progenitor cell could be impaired. The failure of progenitor cells to develop normally could be due to an intrinsic defect in the progenitor cell (cell autonomous), or a defect in the microenvironment in which the progenitor cell develops (cell non-autonomous). Our data can exclude a complete defect in migration of pluripotent hematopoietic stem cells to the fetal liver, but cannot exclude a partial defect at this level. Further studies to evaluate the number of pluripotent stem cells present in *Lhx2–/–* livers need to be completed to exclude a partial defect at this level. However, we have demonstrated a disproportionate effect on maturation of erythropoietic progenitors in the livers of *Lhx2–/–* embryos.

The onset and distribution of *Lhx2* expression in the developing liver suggest that it is expressed in developing lymphoid cells (Xu et al., 1993). We did not detect *Lhx2* expression in mouse erythroleukemia cells using northern blot analysis (data not show); however, expression of *Lhx2* in human erythroleukemia cells was reported by Wu et al. (1996). To ascertain whether the defect in erythropoiesis was cell autonomous or cell non-autonomous, we evaluated the ability of *Lhx2–/–* embryonic stem cells to produce mature erythrocytes in chimeric animals. The proportion of hemoglobin derived from the *Lhx2–/–* embryonic stem cells ranged from 40-80% in eight chimeric

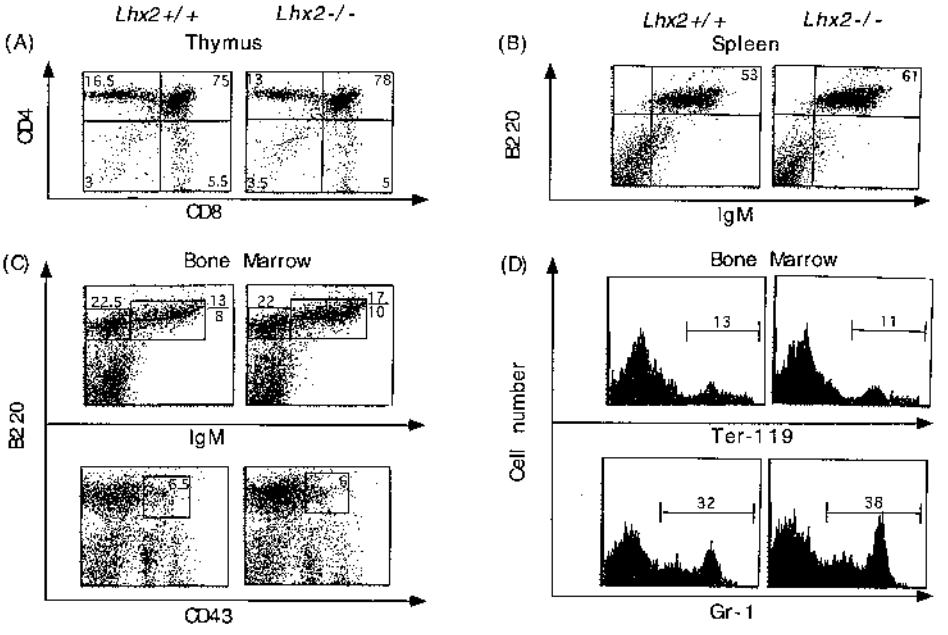

Fig. 6. Flow cytometric analysis of hematopoietic cells in lethally irradiated mice. Fetal liver cells from *Lhx2+/+* and *Lhx2–/–* embryos were transplanted into lethally irradiated mice, and flow cytometric analysis was performed. The antibodies used for staining and tissues analyzed are indicated in the figure. In A,B and C cells residing in the lymphocyte gate were analyzed and the percentage of cells in a particular region is shown. In D bone marrow was analyzed for cells of the erythroid lineage (Ter-119) and granulocytic lineage (Gr-1).

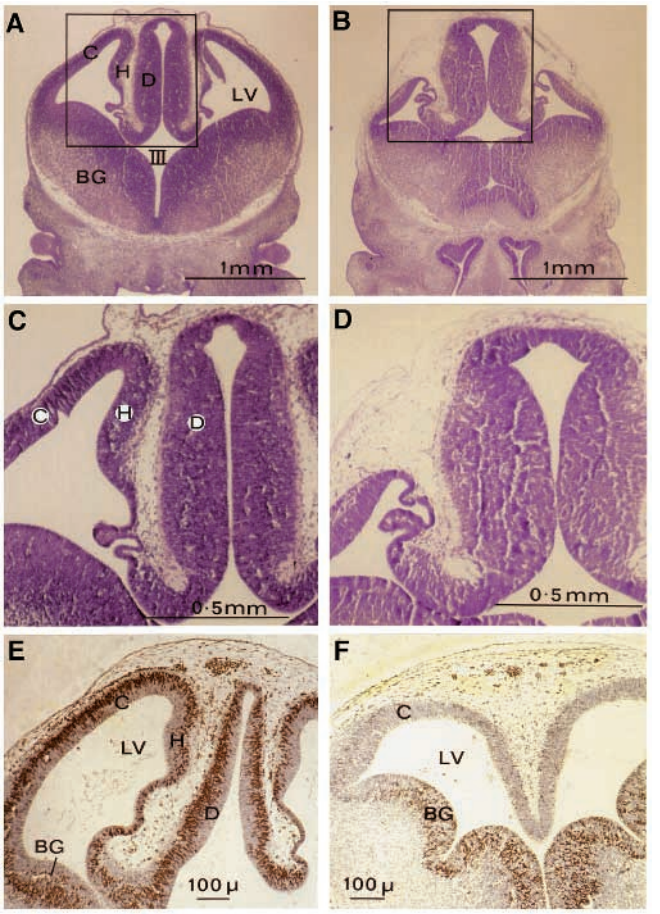

Fig. 7. Hypoplasia of the neocortex and aplasia of the archicortex in *Lhx2–/–* embryos due to a proliferative defect. Cresyl violet stained coronal sections of E12.5 *Lhx2*+/+ (A,C) and *Lhx2–/–* (B,D) embryos demonstrate hypoplasia of the cortical plate and aplasia of the hippocampal anlagen. Cortical plate (C), hippocampal anlagen (H), basal ganglia (BG), third ventricle (III), lateral ventricle (LV), and diencephalon (D). BrdU labeling of mitotic cells was used to define the proliferative defect in the development of the cerebral cortex of *Lhx2–/–* embryos (F) versus *Lhx2*+/+ embryos (E).

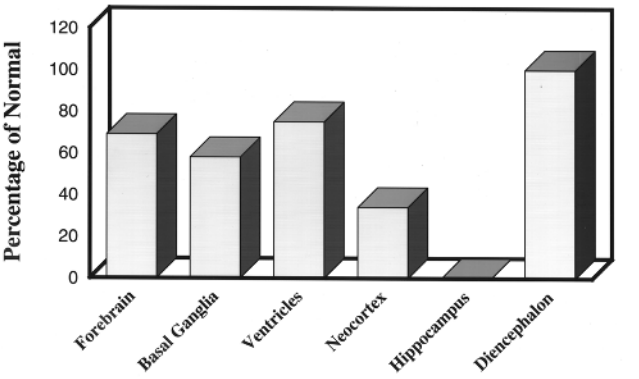

Fig. 8. Morphometric analysis of the forebrain region of *Lhx2*+/+ and –/– embryos. This histogram demonstrates the absence of the hippocampal anlagen and the reductions in the volumes of the forebrain ($P<0.05$), the cortical plate ($P<0.05$), and the basal ganglion anlagen ($P<0.01$) of *Lhx2–/–* embryos ($n=4$) compared to *Lhx2*+/+ embryos. The volumes of the ventricular system and the diencephalon did not differ significantly between *Lhx2*+/+ and –/– embryos at E12.5.

pups. To confirm this observation, *Lhx* 2–/– fetal liver cells were transplanted into lethally irradiated mice. Flow cytometric analysis of Ter-119 expression, a marker of the erythroid lineage, demonstrated that erythropoiesis was reconstituted in the transplanted mice. Thus the erythropoietic defect seen in *Lhx2–/–* embryos was cell non-autonomous and was likely to be due to a defect in the fetal hepatic microenvironment. A cell non-autonomous defect in erythropoiesis has also been observed in *Hlx–/–* embryos (Hentsch et al., 1996). However, in these embryos, definitive erythropoiesis was secondarily impaired due to a defect in viceral organogenesis. In contrast, liver development is grossly normal and proceeds much further in *Lhx2–/–* embryos. In addition development of the gut does not appear to be affected in *Lhx2* mutants. These observations suggests a more limited effect of *Lhx2* on the development of the hepatic microenvironment. We hypothesize that the erythropoietic defect is due to abnormal expression of a *Lhx2* target gene that functions in the extracellular, fetal hepatic microenvironment. Given that the cortical defect in *Lhx2* mutants is due to a defect in cellular proliferation, the lack of a *Lhx2* regulated growth factor could provide a unifying explanation for the pleiotropic phenotype observed. Experiments are now underway to identify the gene targets of *Lhx2* that are ultimately responsible for the failure of definitive erythropoiesis.

Lack of *Lhx2* function results in neocortex hypoplasia and aplasia of the hippocampal anlagen

Lhx2 is expressed widely in the developing central nervous system. In the forebrain expression was observed in the neocortex, archicortex, the basal ganglia, the dorsal thalamus and the hypothalamus. We also observed *Lhx2* expression in the dorsal midbrain and in the rostral hindbrain. In the cerebral cortex, *Lhx2* transcripts are detected in the ventricular, intermediate, and mantle zones; whereas, in the midbrain and hindbrain *Lhx2* expression is limited to the outer layers. In *Lhx2–/–* embryos, we observed a reduction in the size of the cerebral cortex. Specifically, we saw that the neocortex was hypoplastic, and the archicortex (which includes the hippocampal anlagen) was aplastic. BrdU labeling studies and TUNEL staining demonstrated that this decrease in cellular mass was due to decreased proliferation rather than increased cellular death. A similar defect in cellular proliferation of the anterior pituitary was observed in *Lhx3–/–* embryos (Sheng et al., 1996). It is not readily apparent why these two areas of the cerebral cortex are differentially affected in the *Lhx2–/–* embryos. One hypothesis is that a related gene is able to provide partial functional redundancy for *Lhx2* in the neocortex, and that this second gene is not active in the archicortex. Such a situation has been observed with *engrailed-1* and *engrailed-2* in cerebellar development (Hanks et al., 1995), and also for *Lhx3* and *Lhx4* in pituitary development (Sheng and Westphal, unpublished observations). This hypothesis may also explain the apparent lack of a distinct phenotype in the midbrain, the hindbrain, the nasal epithelium and the limbs where *Lhx2* is also expressed. A second hypothesis would be that the function of Lhx2 differs in these two architecturally distinct cortical structures. The aplasia of the hippocampal anlagen may therefore be

a reflection of the interaction of Lhx2 with a second protein that modulates its function and is exclusively expressed in the nascent hippocampus. The recent cloning of a novel family of proteins that binds to and activates LIM homeodomain proteins (Agulnick et al., 1996) supports the idea that Lhx2 in combination with regional specific interacting proteins may have different functions. Further studies to identify a related LIM homeobox gene and to further characterize the interactions of Lhx2 with Lbd family members are needed to differentiate between these two possibilities.

The differential effect of a mutation of *Lhx2* on the development of the neocortex and archicortex provides functional support for the prosomeric model that has been proposed by Puelles and Rubenstein (1993). Their initial model proposed that the archicortex develops from the fourth prosomere, while the neocortex develops from the fifth prosomere. Rubenstein and colleagues (Bulfone et al., 1995) have subsequently advanced two alternative models that take into account the relatively homogeneous expression patterns of a number of genes in the developing cerebral cortex. In these models, both the archicortex and the neocortex are proposed to develop from a single prosomere. Although expression of *Lhx2* crosses the proposed prosomeric boundaries, the development of these two CNS compartments differs in their requirement for Lhx2. Thus the forebrain phenotype of the *Lhx2–/–* embryos supports the initial model that allocates the archicortex and the neocortex to separate prosomeres. Analysis of the expression patterns of other genes proposed to be involved in specification of forebrain compartments will also be useful in further characterizing the possible functional difference for *Lhx2* in the archicortex versus the neocortex.

This study shows that *Lhx2* is essential for normal development of the cerebral cortex. The primary defect appears to be a proliferative block in neuronal precursor cells. Previously, it was hypothesized that the expression of *Lhx2* in the outer layers of the developing cortex is consistent with a role for *Lhx2* in neuronal differentiation (Xu et al., 1993); however, the presence of *Lhx2* transcripts in the outer layer of the cerebral cortex may simply reflect the fact that neuronal precursor cells migrate rapidly after division, or that *Lhx2* functions in both neuronal precursor cell proliferation and in neuronal differentiation. Due to the in utero death of these embryos prior to formation of a mature cortex, we currently cannot address the role of *Lhx2* in the differentiation of neurons. This role and the function of *Lhx2* in the adult cortex and hippocampus awaits development of a mouse model and in vitro systems in which *Lhx2* function can be inhibited in a specific tissue and at a specific time of development.

We would like to thank Keveta Cveklova for her help in genotyping mice, Paul M. Chamberlain for his assistance with the morphometric analysis, and D. Feltner, M. O'Reilly and K. A. Mahon for their comments on this manuscript. John Drago is a Logan Research Fellow and this work is supported by a Wellcome Australian Fellowship, and a National Health and Medical Research of Australia grant.

REFERENCES

Agulnick, A. D., Taira, M., Breen, J. J., Tanaka, T., Dawid, I. B. and Westphal, H. (1996). Interactions of the LIM-domain binding factor Ldb1 with LIM homeodomain proteins. *Nature* **384**, 270-272.

Archer, V. E. V., Breton, J., Sánchez-García, I., Osada, H., Forster, A., Thompson, A. J. and Rabbitts, T. H. (1994). Cysteine-rich LIM domains of LIM-homeodomain and LIM-only proteins contain zinc but not iron. *Proc. Natl. Acad. Sci. USA* **91**, 316-320.

Bach, I., Rhodes, S. J., Pearse II, R. V., Heinzel, T., Gloss, B., Scully, K. M., Sawchenko, P. E. and Rosenfeld, M. G. (1995). P-LIM, a LIM homeodomain factor, is expressed during pituitary organ and cell commitment and synergizes with Pit-1. *Proc. Natl. Acad. Sci. USA* **92**, 2720-2724.

Barnes, J. D., Crosby, J. L., Jones, M. C., Wright, C. V. E. and Hogan, B. L. M. (1994). Embryonic expression of *Lim-1*, the mouse homolog of *Xenopus XLIM-1*, suggests a role in lateral mesoderm differentiation and neurogenesis. *Dev. Biol.* **161**, 168-178.

Bradley, A. (1987). Production and analysis of chimaeric mice. In *Teratocarcinomas and Embryonic Stem Cells: A Practical Approach*, (ed. E. J. Robertson), pp. 113-151.

Bulfone, A., Smiga, S. M., Shimamura, K., Peterson, A., Puelles, L. and Rubenstein, J. L. R. (1995). T-Brain-1: A homolog of Brachyury whose expression defines molecularly distinct domains within the cerebral cortex. *Neuron* **15**, 63-78.

Crawford, A. W., Michelsen, J. W. and Beckerle, M. C. (1992). An interaction between zyxin and α-actinin. *J. Cell Biol.* **116**, 1381-1393.

Dawid, I. B., Toyama, R. and Taira, M. (1995). LIM Domain Proteins. *C. R. Acad. Sci. Paris* **318**, 295-306.

Feuerstein, R., Wang, X., Song, D., Cooke, N. E. and Liebhaber, S. A. (1994). The LIM/double zinc-finger motif functions as a protein dimerization domain. *Proc. Natl. Acad. Sci. USA* **91**, 10655-10659.

Fujii, T., Pichel, J. G., Taira, M., Toyama, R., Dawid, I. B. and Westphal, H. (1994). Expression patterns of the murine LIM class homeobox gene *lim1* in the developing brain and excretory system. *Dev. Dyn.* **199**, 73-83.

Gehring, W. J., Affolter, M. and Burglin, T. (1994). Homeodomain Proteins. *Ann. Rev. Biochem.* **63**, 487-526.

German, M. S., Wang, J., Chadwick, R. B. and Rutter, W. J. (1992). Synergistic activation of the insulin gene by a LIM-homeodomain protein and a basic helix-loop-helix protein: building a functional insulin minienhancer complex. *Genes Dev.* **6,** 2165-2176.

Grainger, R. M. (1992). Embryonic lens induction: shedding light on vertebrate tissue determination. *Trends Genet.* **8,** 349-355.

Halder, G., Callaerts, P. and Gehring, W. J. (1995). Induction of ectopic eyes by targeted expression of the eyeless gene in Drosophila. *Science* **267**, 1788-1792.

Hanks, M., Wurst, W., Anson-Cartwright, L., Auerbach, A. B. and Joyner, A. L. (1995). Rescue of the En-1 mutant phenotype by replacement of En-1 with En-2. *Science* **269**, 679-682.

Hanson, I. and van Heyningen, V. (1995). Pax6: more than meets the eye. *Trends Genet.* **11**, 268-272.

Hentsch, B., Lyons, I., Li, R., Hartley, L., Lints, T. J., Adams, J. M. and Harvey, R. P. (1996) Hlx homeo box gene is essential for an inductive tissue interaction that drives expansion of embryonic liver and gut. *Genes Dev.* **10**, 70-79.

Hill, R. E., Favor, J., Hogan, B. L. M., Ton, C. C. T., Saunders, G. F., Hanson, I. M., Prosser, J., Jordan, T., Hastie, N. D. and van Heyningen, V. (1991). Mouse Small eye results from mutations in a paired-like homeobox-containing gene. *Nature* **354**, 522-525.

Hogan, B. L. M., Horsburgh, G., Cohen, J., Hetherington, C. M., Fisher, G. and Lyon, M. F. (1986). Small eyes (Sey): a homozygous lethal mutation on chromosome 2 which affects the differentiation of both lens and nasal placodes in the mouse. *J. Embryol. Exp. Morph.* **97**, 95-110.

Jurata, L. W., Kenny, D. A. and Gill, G. N. (1996). Nuclear LIM interactor, a rhombotin and LIM homeodomain interacting protein, is expressed early in neuronal development. *Proc. Natl. Acad. Sci. USA* **93**, 11693-11698.

Laird, P. W., Zijderveld, A., Linders, K., Rudnicki, M. A., Jaenisch, R. and Berns, A. (1991). Simplified mammalian DNA isolation procedure. *Nucleic Acids Res.* **19**, 4293.

Li, E., Bestor, T. H. and Jaenisch, R. (1992). Targeted mutation of the DNA methyltransferase gene results in embryonic lethality. *Cell* **69,** 915-926.

Li, H., Witte, D. P., Branford, W. W., Aronow, B. J., Weinstein, M., Kaur, S., Wert, S., Singh, G., Schreiner, C. M., Whitsett, J. A., Scott, W. J. and Potter, S. S. (1994). Gsh-4 encodes a LIM-type homeodomain, is expressed in the developing central nervous system and is required for early postnatal survival. *EMBO J.* **13**, 2876-2885.

Mackem, S. and Mahon, K. A. (1991). Ghox 4. 7: a chick homeobox gene expressed primarily in limb buds with limb-type differences in expression. *Development* **112**, 791-806.

Manak, J. R. and Scott, M. P. (1994). A class act: conservation of homeodomain protein function. *Development* **Supplement,** 61-77.

Mansour, S. L., Thomas, K. R. and Capecchi, M. R. (1988). Disruption of the proto-oncogene int-2 in mouse embryo-derived stem cells: A general strategy for targeting mutations to non-selectable genes. *Nature* **336**, 348-352.

Perez-Alvarado, G. C., Miles, C., Michelsen, J. W., Louis, H. A., Winge, D. R., Beckerle, M. C. and Summers, M. F. (1994). Structure of the carboxy-terminal LIM domain for the cysteine rich protein CRP. *Struc. Biol.* **1**, 388-398.

Pfaff, S. L., Mendelsohn, M., Stewart, C. L., Edlund, T. and Jessell, T. M. (1996). Requirement for LIM homeobox gene Isl1 in motor neuron generation reveals a motor neuron-dependent step in interneuron differentiation. *Cell* **84**, 309-20.

Puelles, L. and Rubenstein, J. L. R. (1993). Expression patterns of homeobox and other putative regulatory genes in the embryonic mouse forebrain suggest a neuromeric organization. *Trends Neurosci.* **16**, 472-479.

Riddle, R. D., Ensini, M., Nelson, C., Tsuchida, T., Jessell, T. M. and Tabin, C. (1995). Induction of the LIM homeobox gene Lmx1 by WNT7a establishes dorsoventral pattern in the vertebrate limb. *Cell* **83**, 631-640.

Robertson, M. S., Schoderbek, W. E., Tremml, G. and Maurer, R. A. (1994). Activation of the glycoprotein hormone alpha-subunit promotor by a LIM-homeodomain transcription factor. *Mol. Cell. Biol.* **14**, 2985-2993.

Russell, E. (1979). Hereditary anemias of the mouse: A review for geneticists. *Adv. Genet.* **20**, 357-459.

Saha, M. S., Servetnick, M. and Grainger, R. M. (1992). Vertebrate eye development. *Current Opin. Genet. Dev.* **2**, 582-588.

Sánchez-García, I., Osada, H., Forster, A. and Rabbitts, T. H. (1993). The cystein-rich LIM domains inhibit DNA binding by the associated homeodomain in Isl-1. *EMBO J.* **12**, 4243-4250.

Sánchez-García, I. and Rabbitts, T. H. (1994). The LIM domain: a new structural motif found in zinc-finger-like proteins. *Trends Genet.* **10**, 315-320.

Schmeichel, K. L. and Beckerle, M. C. (1994). The LIM domain is a modular protein-binding interface. *Cell* **79**, 211-219.

Seidah, N. G., Barale, J. -C., Marcinkiewicz, M., Mattei, M.-G., Day, R. and Chrétien, M. (1994). The mouse homeoprotein mLIM-3 is expressed early in cells derived from the neuroepithelium and persists in adult pituitary. *DNA and Cell Biol.* **13**, 1163-1180.

Shawlot, W. and Behringer, R. R. (1995). Requirement for Lim1 in head-organizer function. *Nature* **374**, 425-430.

Sheng, H. Z., Zhadanov, A. B., Mosinger, B., Fujii, T., Bertuzzi, S., Grinberg, A., Lee, E. J., Huang, S.-P., Mahon, K. A. and Westphal, H. (1996). Specification of pituitary cell linages by the LIM homeobox gene *Lhx3*. *Science* **272**, 921-1068.

Sheng, H. Z., Bertuzzi, S., Chiang, C., Shawlot, W., Taira, M. Dawid, I. and Westphal, H. (1997). Expression of murine Lhx5 suggests a role in specifying the forebrain. *Dev. Dynam.* (in press).

Taira, M., Otani, H., Saint-Jeannet, J.-P. and Dawid, I. B. (1994). Role of the LIM class homeodomain protein XLIM-1 in neural and muscle induction by the Spemann organizer in *Xenopus*. *Nature* **372**, 677-679.

Thor, S., Ericson, J., Brännström, T. and Edlund, T. (1991). The homeodomain LIM protein Isl-1 is expressed in subsets of neurons and endocrine cells in the adult rat. *Neuron* **7**, 881-889.

Tsuchida, T., Ensini, M., Morton, S. B., Baldassare, M., Edlund, T., Jessell, T. and Pfaff, S. L. (1994). Topographic organization of embryonic motor neurons defined by expression of LIM homeobox genes. *Cell* **79**, 957-970.

Vogel, A., Rodriguez, C., Warnken, W. and Belmonte, J. C. I. (1995). Dorsal cell fate specified by chick Lmx1 during vertebrate limb development. *Nature* **378**, 716-720.

Wadman, I., Li, J., Bash, R. O., Forster, A., Osada, H., Rabbitts, T. H. and Baer, R. (1994). Specific *in vivo* association between the bHLH and LIM proteins implicated in human T-cell leukemia. *EMBO J.* **13**, 4831-4839.

Walther, C. and Gruss, P. (1991). Pax-6, a murine paired box gene, is expressed in the developing CNS. *Development* **113**, 1435-1449.

Whitney, J. B. D. (1978). Simplified typing of mouse hemoglobin (Hbb) phenotypes using cystamine. *Biochem. Genet.* **16**, 667-672.

Wu, H-K., Heng, H. H. Q., Siderovski, D. P., Dong, W-F., Okuno, Y., Shi, X-M., Tsui, L-P. and Minden, M. D. (1996). Identification of a human LIM-Hox gene, hLH-2, aberrantly expressed in chronic myelogenous leukaemia and located on 9q33-34.1. *Oncogene* **12**, 1205-1212.

Wu, R. Y. and Gill, G. N. (1994). LIM domain recognition of a tyrosine-containing tight turn. *J. Biol. Chem.* **269**, 25085-25090.

Xu, Y., Baldassare, M., Fisher, P., Rathbun, G., Oltz, E. M., Yancopoulos, G. D., Jessell, T. M. and Alt, F. W. (1993). LH-2: A LIM/homeodomain gene expressed in developing lymphocytes and neural cells. *Proc. Natl. Acad. Sci. USA* **90**, 227-231.

Xu, Y., Davidson, L., Alt, F. W. and Baltimore, D. (1996). Deletion of the Ig kappa light chain intronic enhancer/matrix attachment region impairs but does not abolish V kappa J kappa rearrangement. *Immunity* **4**, 377-385.

Xue, D., Tu, Y. and Chalfie, M. (1993). Cooperative interactions between the *Caenorhabditis elegans* homeoproteins UNC-86 and MEC-3. *Science* **261**, 1324-1328.

Zhadanov, A., Bertuzzi, S., Taira, M., Dawid, I. B. and Westphal, H. (1995). Expression pattern of the murine LIM class homeobox gene Lhx3 in subsets of neural and neuroendocrine tissues. *Dev. Dyn.* **202**, 354-364.

(Accepted 20 May 1997)